

QSAN: A Near-term Achievable Quantum Self-Attention Network

Ren-xin Zhao¹, Jinjing Shi¹, Shichao Zhang¹

¹ School of Computer Science and Engineering, Central South University, Changsha, China

Abstract—Self-Attention Mechanism (SAM), an important component of machine learning, has been relatively little investigated in the field of quantum machine learning. Inspired by the Variational Quantum Algorithm (VQA) framework and SAM, Quantum Self-Attention Network (QSAN) that can be implemented on a near-term quantum computer is proposed. Theoretically, Quantum Self-Attention Mechanism (QSAM), a novel interpretation of SAM with linearization and logicalization is defined, in which Quantum Logical Similarity (QLS) is presented firstly to impel a better execution of QSAM on quantum computers since inner product operations are replaced with logical operations, and then a QLS-based density matrix named Quantum Bit Self-Attention Score Matrix (QBSASM) is deduced for representing the output distribution effectively. Moreover, QSAN is implemented based on the QSAM framework and its practical quantum circuit is designed with 5 modules. Finally, QSAN is tested on a quantum computer with a small sample of data. The experimental results show that QSAN can converge faster in the quantum natural gradient descent framework and reassign weights to word vectors. The above illustrates that QSAN is able to provide attention with quantum characteristics faster, laying the foundation for Quantum Natural Language Processing (QNLP).

Index Terms—Quantum Self Attention Mechanism, Quantum Circuit, Quantum Natural Language Processing, Quantum Machine Learning, Quantum Network.

I. INTRODUCTION

SAM is a powerful component embedded in machine learning models that reduces the dependence on external information and better captures the intrinsic relevance of data or features, thus significantly enhancing the performance of the model. It was originally introduced by a deep learning framework for machine translation called Transformer [1], and now is extensively employed in Natural Language Processing (NLP) [2], Speech [3], and Computer Vision [4].

Although SAM is very beneficial, its complexity escalates quadratically with the length of the input sequence, severely hindering its exploration on longer sequences. Some proposals, such as Nystrom matrix decomposition [5], kernel methods [6, 7], hashing strategies [8], sparsification [9–11], linearization [12], etc., have good effect in diminishing the complexity. In further, Ref. [13] identified the limitation of the SAM that it is unable to model periodic finite state languages and hierarchical constructions, with a fixed number of layers or

heads. Perhaps exploring structural adaptive SAM could bring new opportunities to this challenge.

On the other hand, quantum computer is considered as a promising processor paradigm that surpasses the limits of traditional computer computing and have made significant breakthroughs in recent years [14–16]. The superiority offered by quantum computers, also known as quantum supremacy, specifically refers to the exponential storage and secondary computational acceleration arising from the effects of quantum properties [17, 18]. Ref. [19] exploited the idea of weak measurement in quantum mechanics to construct a parameter-free, more efficient quantum attention, which is used in the LSTM framework and found to have better sentence modeling performance. Ref. [20] understood the quantum attention mechanism as a density matrix by which more powerful sentence representations can be constructed. Unfortunately, the above two approaches only involve certain physical concepts in quantum mechanics without feasibility on quantum processors. A recent meaningful effort was contributed by the Baidu group. A Gaussian projection-based QSAN using VQA [21–31] to build Parametric Quantum Circuits (PQC) on NISQ [32] devices was applied to text classification [33]. Nevertheless, obviously this model does not accomplish all the tasks on a quantum computer; instead, subsequent weighting operations must be carried out on a classical computer in order to yield the ultimate output.

Inspired by [1, 21], a novel QSAN is formally presented as an attempt to address the fact that the high complexity of SAM will consume more storage and that QSAM still lacks diverse research. Compared to SAM, QSAM demands exponentially less storage than SAM with the help of quantum representation for the same input sequence. In contrast to Ref. [19, 20, 33], QSAN is fully deployed and realized on quantum devices with fewer measurements and a beneficial byproduct called QBSASM. But the essential motivation for proposing QSAN is to explore whether young quantum computers can have quantum characteristic attention and can depict the distribution of outputs in a quantum language, not to replace SAM or to beat all the schemes in the Ref. [19, 20, 33]. Quantum characteristic here should be understood as probability, linearity and reversibility, while the quantum language should refer to specialized terms in quantum mechanics, such as density matrix, Hamiltonian operators, etc. To this end, the following efforts are made.

- ★ A theoretical framework QSAM: QSAM is a new attempt to linearize, reversiblize and logicalize SAM.
- ★ Two key ideas QLS and QBSASM in QSAM: QLS

Ren-xin Zhao and Jinjing Shi is with School of Computer Science and Engineering, Shaoshan South Road, Tianxin District, Changsha City, Hunan Province, China. (e-mail:13061508@alu.hdu.edu.cn; shijinjing@csu.edu.cn)

Corresponding author: Jinjing Shi.

replaces inner product operations with logical operations, avoiding the construction of large numerical operations, saving more auxiliary qubits and improving feasibility. QBSASM is a useful by-product based on QLS, depicting the distribution of the output in the form of a density matrix.

- ★ An achievable model QSAN and a guideline for efficient design, quantum coordinates: for regular circuit layouts, quantum coordinates establish a functional dependence for quantum control bits and output bits. Once this function is found, the positions of all control bits and output bits can be known, facilitating programming and opening a path to optimization. Guided by QSAM theory and quantum coordinates, 5 quantum subcircuits are specially designed so that QSAN can be fully deployed and executed on a quantum computer with fewer measurements.

This paper is organized as follows. In Section II, some basics are reviewed. In Section III, QLS, QBSASM and QSAM are described, which are the theoretical basis for the birth of QSAN. In Section IV, the potential of quantum coordinates and the design of QSAN are explained. In Section V, the results of a small sample test of QSAN in the IBM qiskit and pennylane environments are displayed, and some useful discussions are made. Finally, a summary is made.

II. PRELIMINARIES

This section briefly outlines SAM, VQA, and quantum operators. First a protocol is made for subscripts: if not specifically stated in this paper, subscripts always denote the sequence number of the variable.

A. Self Attention Mechanism

The input set $\mathbf{In} = \{\mathbf{w}_0, \dots, \mathbf{w}_{n-1}\}$ and the output set $\mathbf{Out} = \{\mathbf{new_w}_0, \dots, \mathbf{new_w}_{n-1}\}$ are defined, where any element \mathbf{w}_i as well as $\mathbf{new_w}_j$ with $i, j \in \{0, \dots, n-1\}$ is a vector of dimension l , n is regarded as the total number of word vectors. Then SAM [1] can be stated as

$$\mathbf{new_w}_i = \sum_j \text{softmax} \left(\frac{\mathbf{Q}_i \mathbf{K}_j^T}{\sqrt{d}} \right) \mathbf{V}_j. \quad (1)$$

In Eq. (1), \sqrt{d} is a scaling factor. $\mathbf{Q}_i, \mathbf{V}_j$ are row vectors, where

$$\mathbf{Q}_i = U_Q \cdot \mathbf{w}_i,$$

$$\mathbf{V}_j = U_V \cdot \mathbf{w}_j,$$

\mathbf{w}_i and \mathbf{w}_j are inputs. \mathbf{K}_j^T is a column vector, which is the transpose of

$$\mathbf{K}_j = U_K \cdot \mathbf{w}_j.$$

U_Q, U_K, U_V are three trainable parameter matrices named as query matrix, key matrix and value matrix respectively. The weights

$$\text{softmax} \left(\frac{\mathbf{Q}_i \mathbf{K}_j^T}{\sqrt{d}} \right),$$

also called attention scores, are obtained by normalizing the inner product $\mathbf{Q}_i \mathbf{K}_j^T$. $\mathbf{new_w}_i$ represents new word vector after the weighting operation.

B. Variational Quantum Algorithm

In the NISQ era, it is very difficult to fully deploy deep networks for deep learning on quantum computers with limited qubits. On the one hand, the dimensionality of the model grows exponentially as the size of the quantum circuit gets larger [22]. On the other hand, noise imposes many unknowns on the training results [23]. Therefore, quantum-classical hybrid models can be deemed as an efficient path. VQA is one such class of algorithms. Fig. 1 exhibits the framework of VQA, which can be divided into two parts.

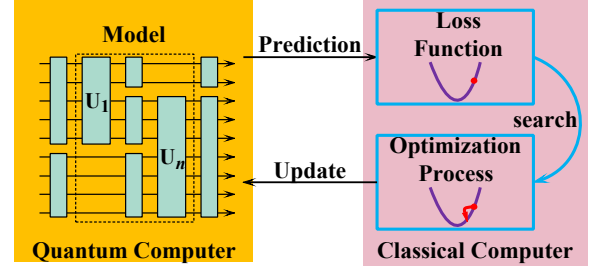


Fig. 1: Framework of VQA

1. The pink box designates the range of the classical computer. This stage focuses on the calculation of the loss function and the optimization of the parameters, as shown in the two purple curves in Fig. 1. The general formulation of the loss function is:

$$C(\theta) = \sum_k f_k(\text{Tr}[O_k U(\theta)] \rho_k U^\dagger(\theta)) \quad (2)$$

where f_k is a set of certain functions determined by specific tasks. $U(\theta) = \otimes_i U_i(\theta_i)$ denotes the product of a series of unitary operators, where θ comprises a series of continuous or discrete hyperparameters. $\{\rho_k\}$ is the input state of the training set, and O_k is a set of observables. Some strategies for training loss functions can be consulted in [24–26].

2. The tan box stands for the quantum computer domain. In this box, a PQC model is drawn. The black dashed box is the centerpiece of this model, the Ansatz, which is a circuit with a specific structure and function. Common examples of Ansatz contain hardware-efficient Ansatz (a quantum circuit model that decreases the circuit depth required to implement $U(\theta)$ for a given quantum hardware) [27, 28], quantum alternating operator Ansatz (can searches for optimal solutions to combinatorial optimization problems) [29–31], etc.

The arrows in the figure illustrate the interaction of information between a quantum computer and a classical computer. The quantum computer provides the classical computer with quantum circuit measurements and loss function forms to be used for prediction. After the classical computer is trained, a new round of hyperparameters is uploaded and updated into the quantum circuit.

C. Qubit and Operators

The smallest unit of information in a quantum computer is a qubit $|\psi\rangle$ which can be represented as a linear superposition of two eigenstates $|0\rangle$ and $|1\rangle$, namely

$$|\psi\rangle = \alpha|0\rangle + \beta|1\rangle,$$

where α and β are probability amplitudes and satisfy

$$|\alpha|^2 + |\beta|^2 = 1.$$

These qubits evolve through unitary operators U which are also called quantum gates and refer to matrices that satisfy

$$U = U^\dagger \\ UU^\dagger = \mathbb{I}$$

where U^\dagger is the complex conjugate of U . This article mainly uses Rotating Pauli Y Gate

$$R_y(\theta) = \begin{pmatrix} \cos(\theta/2) & -\sin(\theta/2) \\ \sin(\theta/2) & \cos(\theta/2) \end{pmatrix},$$

Hadamard Gate

$$H = \frac{1}{\sqrt{2}} \begin{pmatrix} 1 & 1 \\ 1 & -1 \end{pmatrix},$$

SWAP gate

$$SWAP = \begin{pmatrix} 1 & 0 & 0 & 0 \\ 0 & 0 & 1 & 0 \\ 0 & 1 & 0 & 0 \\ 0 & 0 & 0 & 1 \end{pmatrix},$$

CNOT gate

$$CNOT = \begin{pmatrix} 1 & 0 & 0 & 0 \\ 0 & 1 & 0 & 0 \\ 0 & 0 & 0 & 1 \\ 0 & 0 & 1 & 0 \end{pmatrix},$$

and Toffoli gate

$$Toffoli = \begin{pmatrix} 1 & 0 & 0 & 0 & 0 & 0 & 0 & 0 \\ 0 & 1 & 0 & 0 & 0 & 0 & 0 & 0 \\ 0 & 0 & 1 & 0 & 0 & 0 & 0 & 0 \\ 0 & 0 & 0 & 0 & 0 & 0 & 0 & 1 \\ 0 & 0 & 0 & 0 & 1 & 0 & 0 & 0 \\ 0 & 0 & 0 & 0 & 0 & 1 & 0 & 0 \\ 0 & 0 & 0 & 0 & 0 & 0 & 1 & 0 \\ 0 & 0 & 0 & 1 & 0 & 0 & 0 & 0 \end{pmatrix}.$$

III. QUANTUM SELF-ATTENTION MECHANISM

This section presents a logicalized, linearized QSAM framework in which QLS is used to measure logical similarity and enables QSAM to be freed from numerical operations such as addition, thus conserving more qubits. More importantly QLS replaces the inner product similarity that needs to be implemented by measurement, which ensures that the task is always executed on the quantum computer without interruption. QBSASM derived from QLS expresses the weight distribution of the quantum computer on word vectors in the form of a density matrix.

Before starting, first the sets **In** and **Out** are re-expressed in quantum states as $\mathbf{Q}_{in} = \{|\mathbf{w}_0\rangle, \dots, |\mathbf{w}_{n-1}\rangle\}$ and $\mathbf{Q}_{out} = \{|\mathbf{new_w}_0\rangle, \dots, |\mathbf{new_w}_{n-1}\rangle\}$ respectively, where each element $|\mathbf{w}_a\rangle, a \in \{0, \dots, n-1\}$ of \mathbf{Q}_{in} is a vector of dimension $m = \lceil \log_2 l \rceil$, and l is the feature dimension of the classical word vector. The dimension of $|\mathbf{new_w}_b\rangle, b \in \{0, \dots, n-1\}$ is higher, mainly because QSAM is described as

$$|\mathbf{new_w}_i\rangle := \bigoplus_j \langle \mathbf{Q}_i | \mathbf{K}_j \rangle \otimes |\mathbf{V}_j\rangle. \quad (3)$$

In Eq. (3),

$$|\mathbf{Q}_i\rangle = U_q |\mathbf{W}_i\rangle, \quad (4)$$

$$|\mathbf{K}_j\rangle = U_k |\mathbf{W}_j\rangle, \quad (5)$$

$$|\mathbf{V}_j\rangle = U_v |\mathbf{W}_j\rangle, \quad (6)$$

where U_q , U_k and U_v are specified as three composite unitary operators with the identical structure but distinct parameters. The same composition means that all three matrices above are composed of $(m-1)$ Hadamard gates, m rotating Pauli Y gates, and m CNOT gates, and are arranged in order

$$U_{M \in \{q,k,v\}} = CNOT^{\otimes(m-1)} R_y(\theta_M)^{\otimes m} H^{\otimes m}. \quad (7)$$

The benefit of this design is to maintain that the probability amplitudes are all real numbers [38]. Furthermore, $|\mathbf{w}_i\rangle$ and $|\mathbf{w}_j\rangle$ are input word vectors. The symbol \otimes signifies a tensor operation. $\langle \mathbf{Q}_i | \mathbf{K}_j \rangle$ is a QLS that will be introduced next. The symbol \odot encompasses two operations. One is to apply a multi-controlled CNOT gates to QLS to get the logical sum of a particular QLS. The method of getting specific QLS is called Slicing and will be explained below. The other is to use CNOT gates to $|\mathbf{V}_j\rangle$ to perform dimensional compression.

Formally, Eq. (3) is very similar to Eq. (1), but there are essential changes. Comparing Eq. (1) and Eq. (3), Eq. (1) is an attention mechanism with nonlinear operations, while Eq. (3) has a linearized, logical character, which makes it easier to be implemented on quantum computers across the board. Furthermore, in Eq. (1), a large number of numerical operations are required, such as solving the inner product as well as weighted summation, which is costly to implement on existing quantum computers. In contrast, Eq. (3) reduces the implementation cost with QLS and saves even more qubits.

A. Quantum Logical Similarity

In quantum computing, a common way to characterize the similarity between two quantum states $|\mathbf{Q}_a\rangle$ and $|\mathbf{K}_b\rangle$ is SWAP test [34] or Hadamard test [35]. However, these two schemes are made by multiple measurements to obtain the inner product of quantum states. Yet, the goal of QSAN is not to obtain the similarity between quantum states, but to construct new word vectors with the help of similarity. Therefore, the classical method of using inner product as similarity must be modified.

Definition 1 (QLS): For any quantum state $|\mathbf{Q}_a\rangle$ and $|\mathbf{K}_b\rangle$ with $a, b \in \{0, \dots, n-1\}$, QLS is redefined as

$$\langle \mathbf{Q}_a | \mathbf{K}_b \rangle := \bigoplus_j (\mathcal{Q}_{a,j} \wedge \mathcal{K}_{b,j}) \quad (8)$$

where $|\mathcal{Q}_{a,j}\rangle$ and $|\mathcal{K}_{b,j}\rangle, j \in \{0, \dots, m-1\}$ denote the j -th qubit of $|\mathbf{Q}_a\rangle$ and $|\mathbf{K}_b\rangle$, respectively. The symbol \oplus indicates modulo-two addition and the symbol \wedge is logical AND operation. Eq. (8) may seem counter-intuitive, but in fact, an AND operation can be performed between two superposition states, and the consequence is also a superposition state. From the implementation point of view, AND operation and modulo-two addition can be realized with Toffoli gates and CNOT gates,

respectively. Eq. (8) is then explained in terms of quantum gates:

$$\begin{aligned} & \text{Toffoli}|\mathcal{Q}_{a,j}, \mathcal{K}_{b,j}, 0\rangle \\ &= |\mathcal{Q}_{a,j}, \mathcal{K}_{b,j}, \mathcal{Q}_{a,j} \wedge \mathcal{K}_{b,j}\rangle \\ & \text{CNOT}|\mathcal{Q}_{a,j} \wedge \mathcal{K}_{b,j}, \mathcal{Q}_{a,i} \wedge \mathcal{K}_{b,i}\rangle \\ &= |\mathcal{Q}_{a,j} \wedge \mathcal{K}_{b,j}, (\mathcal{Q}_{a,i} \wedge \mathcal{K}_{b,i}) \oplus (\mathcal{Q}_{a,j} \wedge \mathcal{K}_{b,j})\rangle. \end{aligned}$$

Moreover, Eq. (8) is obviously consistent with the commutation law, i.e.

$$\langle \mathbf{Q}_a | \mathbf{K}_b \rangle = \langle \mathbf{K}_b | \mathbf{Q}_a \rangle,$$

which contributes to computational efficiency and avoidance of barren plateaus due to heavy entanglement [36, 37]. This property demonstrates that Eq. (8) involves the calculation of only $m \sum_{i=1}^n i$ QLS rather than n^2 .

B. Quantum Bit Self-Attention Score Matrix

The procedure for solving the quantum circuit for a single new word vector only is given by Eq. (3). The solution process for all word vectors is redescribed by the matrix as follows:

$$\begin{aligned} & \begin{pmatrix} (\langle \mathbf{Q}_0 | \mathbf{K}_0 \rangle \otimes |\mathbf{V}_0\rangle) \odot \cdots \odot (\langle \mathbf{Q}_0 | \mathbf{K}_{n-1} \rangle \otimes |\mathbf{V}_{n-1}\rangle) \\ (\langle \mathbf{Q}_1 | \mathbf{K}_0 \rangle \otimes |\mathbf{V}_0\rangle) \odot \cdots \odot (\langle \mathbf{Q}_1 | \mathbf{K}_{n-1} \rangle \otimes |\mathbf{V}_{n-1}\rangle) \\ \vdots \\ (\langle \mathbf{Q}_{n-1} | \mathbf{K}_0 \rangle \otimes |\mathbf{V}_0\rangle) \odot \cdots \odot (\langle \mathbf{Q}_{n-1} | \mathbf{K}_{n-1} \rangle \otimes |\mathbf{V}_{n-1}\rangle) \end{pmatrix} \\ &= \begin{pmatrix} | \text{new_word}_0 \rangle \\ | \text{new_word}_1 \rangle \\ \vdots \\ | \text{new_word}_{n-1} \rangle \end{pmatrix}. \end{aligned} \quad (9)$$

The weight coefficient matrix QBSASM

$$\begin{pmatrix} \langle \mathbf{Q}_0 | \mathbf{K}_0 \rangle & \langle \mathbf{Q}_0 | \mathbf{K}_1 \rangle & \cdots & \langle \mathbf{Q}_0 | \mathbf{K}_{n-1} \rangle \\ \langle \mathbf{Q}_1 | \mathbf{K}_0 \rangle & \langle \mathbf{Q}_1 | \mathbf{K}_1 \rangle & \cdots & \langle \mathbf{Q}_1 | \mathbf{K}_{n-1} \rangle \\ \vdots & \vdots & \ddots & \vdots \\ \langle \mathbf{Q}_{n-1} | \mathbf{K}_0 \rangle & \cdots & \cdots & \langle \mathbf{Q}_{n-1} | \mathbf{K}_{n-1} \rangle \end{pmatrix}, \quad (10)$$

is extracted from Eq. (9) to depict the distribution of the output, where each element is computed by QLS. The slicing operation mentioned previously comes into play here. Specifically, slicing takes the element QLS in each row of QBSASM as control bits and uses the result of the AND operation on these elements as a new weight, thus reflecting the weighting operation of QSAN. QBSASM is SAM as a valuable by-product of QSAN, which can be acquired by way of pennylane intercepting the density matrix of QLS.

In summary, the element QLS is a single qubit in the superposition state. Therefore, the dimensionality of the QBSASM is much higher than the classical attention score matrix, which reflects the quantum nature of the QBSASM. Particularly, as the dimensionality increases QBSASM is more difficult to simulate classically, which is manifesting the storage advantage of quantum computers. Finally, it can be known that the output and input of Eq. (3) do not have the same dimensionality, but there is no need to worry about this. The output dimensionality can be effectively controlled using a layer of neural networks, but this is beyond the scope of this paper.

IV. QUANTUM SELF-ATTENTION NETWORK

In this section, the overall framework and quantum circuits of QSAN are illustrated. Especially, a prototype of quantum coordinates is presented, which is a design guideline for quantum circuits with regular layout. With the guidance of quantum coordinates, the functional link between control bits and output bits can be established to facilitate programming. It is also worth exploring in quantum circuit optimization.

A. Framework of Quantum Self-Attention Network

The main framework of QSAN, as shown in Fig. 2, consists of one input register and three garbage registers for computing the query quantum state $|\mathbf{Q}\rangle$, the key quantum state $|\mathbf{K}\rangle$ and QLS. In terms of resource consumption, the first, second and third registers take $n \times m$ qubits each, while the fourth register needs $m \sum_{i=1}^n i$ qubits, for a total of $3m \times n + m \sum_{i=1}^n i$ qubits. Additionally, a trick that can be controlled by the code, i.e., keeping the inputs of the first three registers the same, needs to be noted. In Fig. 2, those with the same operation, such as Step 1, 3, and 6, are marked with the same color. The input here is denoted as $|\mathbf{In}\rangle$, and the output through U_v is represented as the value quantum state $|\mathbf{V}\rangle$.

B. Quantum Coordinates

In order to discover the mathematical connection between the control bits and the output bits, the prototype of quantum coordinates is hereby proposed.

Definition 2 (Quantum Coordinates): For a regularly arranged quantum circuit, the intersection of the number of layers and the circuit line number is the quantum coordinate. Meanwhile, a mathematical general term is satisfied between the coordinates where the control bits (or output bits) of the same class of quantum gates located in two adjacent layers.

Based on the above definition, it is even possible to derive the coordinates of the entire network. Then the whole quantum network will be displayed in the form of coordinate points or can be generalized in a generalized term formula, which enhances the interpretability of the network. The induction by means of coordinate points or generalized terms may provide a feasible solution for quantum circuit optimization. Later on, the charm of quantum coordinates will be exhibited.

Here, a CNOT gate coordinate law applicable to this project is extracted, which will play an important role subsequently. In the same register, the quantum coordinate of the CNOT gate is

$$\text{CNOT}[s(t), s(t) + 1] \quad (11)$$

where

$$s(t) = m \times \frac{t - t \bmod (m-1)}{m-1} + t \bmod (m-1) \quad (12)$$

is a general term formula with respect to t . This expression is more concise. The logical function it implies is to XOR the $s(t)$ -th and $(s(t) + 1)$ -th in the same register. The value range of t depends on the situation.

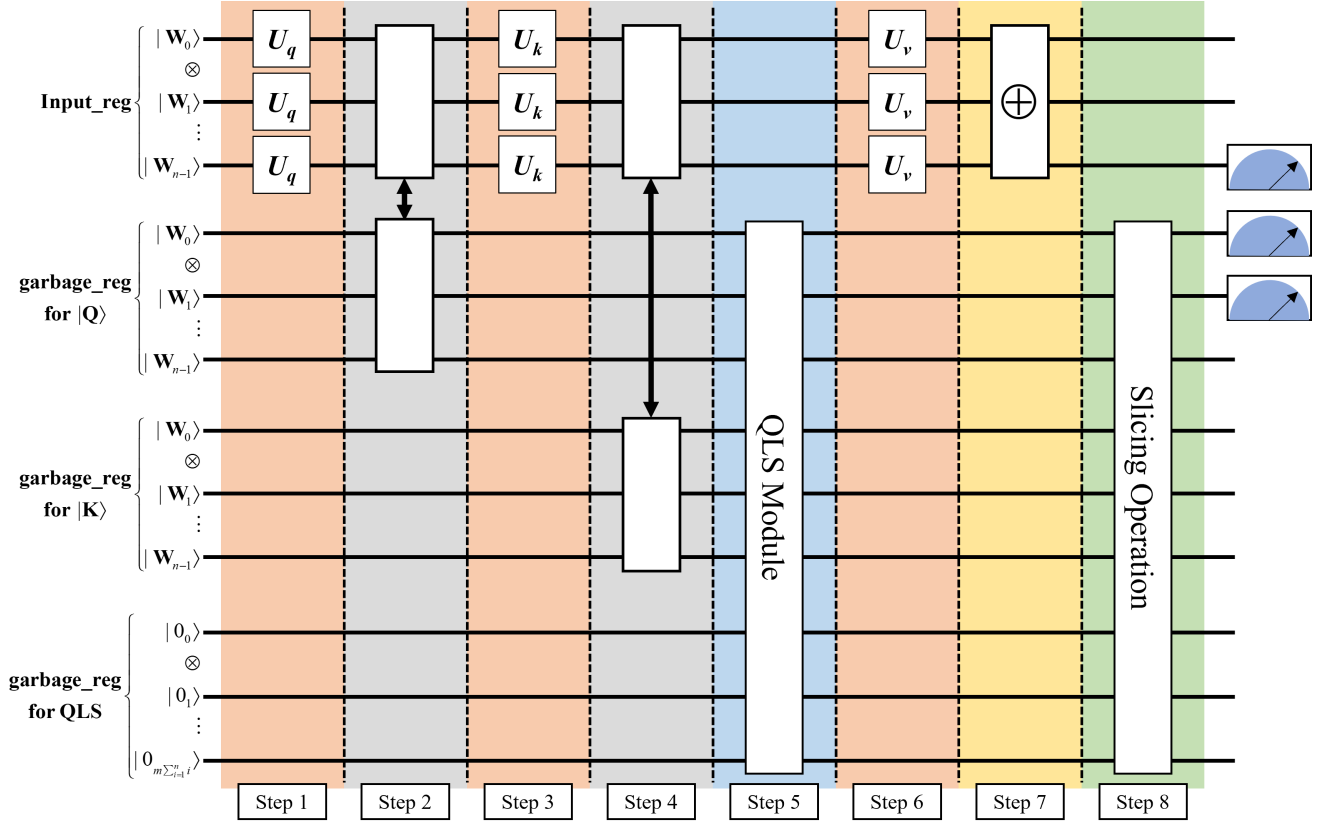


Fig. 2: Circuit Model of QSAN. Step 1, 3 and 6 are dedicated to calculate the query quantum state, the key quantum state and the value quantum state, respectively. Steps 2 and 4 are barbell operations and are designed to swap with the corresponding garbage registers. Step 5 is the QLS module to compute the QLS elements, which will produce the by-product QBSASM. step 7 is the entanglement compression operation, which will reduce the measurements. Step 8 is the slicing operation for calculating the final weights.

C. Quantum Circuit

Step 1: calculate the query quantum state $|Q\rangle$ according to Eq. (4). The procedure is as follows.

$$|U_q^{\otimes n} \text{In, In, In, } 0\rangle = |Q, \text{In, In, } 0\rangle,$$

where $U_q^{\otimes n}$ is shown in Fig. 3 in the order provided by Eq. (7).

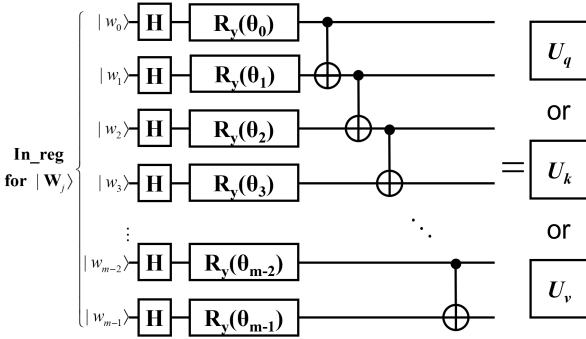


Fig. 3: Circuit for U_q or U_k or U_v

Step 2: perform a barbell operation. The barbell operation, which gets its name from the module's form factor, actually swaps the input value of the second garbage register with the

current value of the input register. This operation causes the input register to be reset and the result of the calculation to be saved in the second garbage register. The exact procedure is explained by the following equation:

$$SWAP^{\otimes(m \times n)} |Q, \text{In, In, } 0\rangle = |\text{In, } Q, \text{In, } 0\rangle,$$

where $SWAP^{\otimes(m \times n)}$ as shown in Fig. 4 indicates that the SWAP gate must be used for each dimension of each word vector.

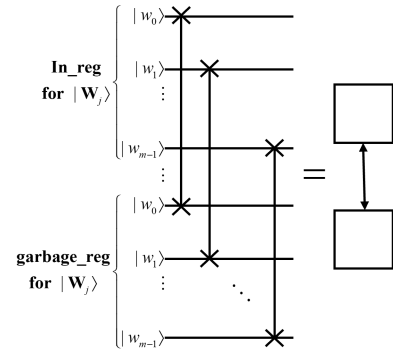


Fig. 4: Circuit for barbell operation

Step 3: calculate the key quantum state $|K\rangle$ according to

Eq. (5). The details are shown in Fig. 3. The mathematical equation is expressed as

$$|U_k^{\otimes n} \text{In}, \mathbf{Q}, \text{In}, \mathbf{0}\rangle = |\mathbf{K}, \mathbf{Q}, \text{In}, \mathbf{0}\rangle.$$

Step 4: perform a barbell operation. This time the current value of the input register is exchanged with the input value of the third register:

$$\text{SWAP}^{\otimes(m \times n)} |\mathbf{K}, \mathbf{Q}, \text{In}, \mathbf{0}\rangle = |\text{In}, \mathbf{Q}, \mathbf{K}, \mathbf{0}\rangle.$$

Step 5: calculate the QLS according to Eq. (8). The details are drawn in Fig. 5.

Firstly, the AND operation is conducted on the qubits in the same position of $|\mathbf{Q}\rangle$ and $|\mathbf{K}\rangle$, and the result is stored in the last garbage register:

$$\text{Tofoli}^{\otimes(m \sum_{i=1}^n i)} |\text{In}, \mathbf{Q}, \mathbf{K}, \mathbf{0}\rangle = |\text{In}, \mathbf{Q}, \mathbf{K}, \mathbf{Q} \wedge \mathbf{K}\rangle.$$

Using the coordinates, $\mathbf{Q} \wedge \mathbf{K}$ is defined as

$$\mathbf{Q} \wedge \mathbf{K} := \otimes_{t,j} \text{Tofoli}[p_1(t), p_2(t), p_3(t, j)] \quad (13)$$

where

$$p_1(t) = t + m \times n,$$

$$p_2(t) = t + 2m \times n,$$

$$p_3(t, j) = t + m \times j + m \left(\sum_{c=1}^{n-1} c - \sum_{d=1}^{n-1-\lfloor t/m \rfloor} d \right) + 3m \times n$$

with $t \in \{0, \dots, m \times n - 1\}$ and $j \in \{0, \dots, n - \lfloor t/m \rfloor - 1\}$.

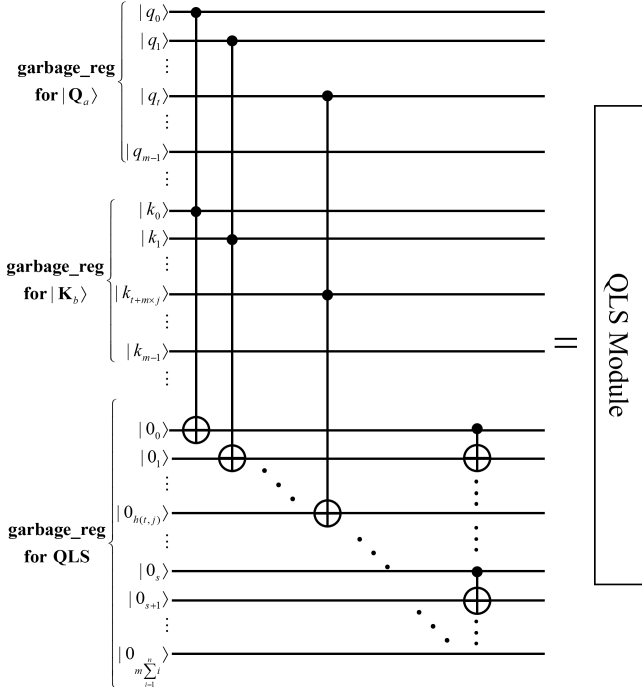


Fig. 5: Circuit for QLS module

Secondly, the CNOT gates are applied to the fourth garbage register to acquire the eventual result of LQS. According to

the law summarized in Eq. (11), the process of applying a CNOT gate at this point is defined as

$$\otimes_t \text{CNOT}[s(t) + 3m \times n, s(t) + 3m \times n + 1],$$

where $t \in \{0, \dots, (m-1) \sum_{i=1}^n i\}$. The fourth register can be located by adding bias $3m \times n$.

The above two steps complete the whole operation steps of QLS:

$$|\text{In}, \mathbf{Q}, \mathbf{K}, \langle \mathbf{Q} | \mathbf{K} \rangle\rangle$$

But the fact is that the outputs $(s(t) + 3m \times n + 1)$ of QLS do not all need to be concerned.

$$g(o) = m \times o - 1 + 3m \times n \in (s(t) + 3m \times n + 1) \quad (14)$$

with $o \in \{1, \dots, \sum_{i=1}^n i\}$ is picked as the true QLS output.

Once the effective outputs $g(o)$ of QLS are available, the distribution of the outputs can be accessed by programmatically querying the density matrix of $g(o)$, i.e., the by-product QBSASM.

Step 6: calculate the key quantum state $|\mathbf{V}\rangle$ according to Eq. (6) and Fig. (3):

$$|U_v^{\otimes n} \text{In}, \mathbf{Q}, \mathbf{K}, \langle \mathbf{Q} | \mathbf{K} \rangle\rangle = |\mathbf{V}, \mathbf{Q}, \mathbf{K}, \langle \mathbf{Q} | \mathbf{K} \rangle\rangle$$

Step 7: The entanglement compression operation, as shown in Fig. 6, means that the output is compressed to the last word vector output of the input register after entanglement by CNOT gates to reduce the number of measurements.

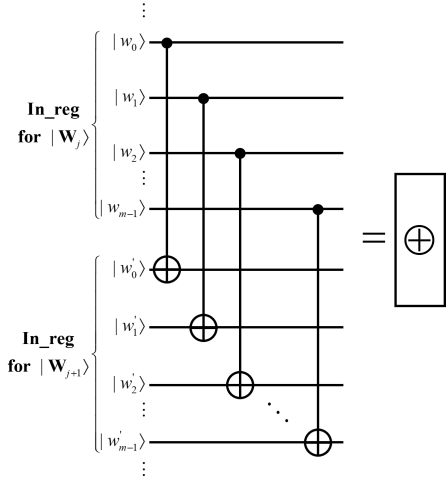


Fig. 6: Circuit for entanglement compression operation

CNOT gates are added for $|\mathbf{V}\rangle$. The specific way of adding CNOT is executed according to Eq. (3) and Eq. (9). Specifically,

$$\text{CNOT}^{\otimes(m \times n)} |\mathbf{V}\rangle = \bigotimes_{i=0}^{m-1} \bigoplus_{j=0}^{n-1} \mathcal{V}_{i,i+m \times j} \quad (15)$$

if $|\mathbf{V}_i\rangle$ is written as

$$|\mathbf{V}_i\rangle = |\mathcal{V}_{i,0} \dots \mathcal{V}_{i,m-1}\rangle$$

where $|\mathcal{V}_{i,j}\rangle$ indicates the j -th qubit of the i -th word vector.

Step 8: execute the slicing operation as shown in Fig. (7) and select the control bits in accordance with Eq. (10).

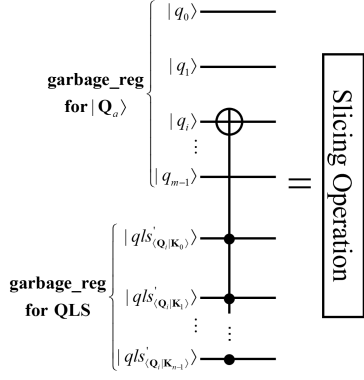


Fig. 7: Circuit for slicing operation

First of all, for Fig. (7), the Reset operation [39] must be performed before applying the multi-control quantum gate, which does not allow $|Q\rangle$ to have any further effect on the output result. Secondly, the relationship between the element $\langle Q_{j_1} | K_{j_2} \rangle$ of QBSASM and the coordinate $g(o)$ is explored, where j_1 is the row number and j_2 is the column number.

Observing Eq. (10) and Eq. (14), it is found that the weight matrix is a symmetric matrix and has the following relationship with the parameter o of Eq. (14):

$$o = \begin{cases} 1 + \sum_{i=1}^n i - \sum_{j=1}^{n-j_1} j + j_2 & j_1 \leq j_2 \\ j_1 + 1 + \sum_{i=1}^{n-1} i - \sum_{j=1}^{n-1-j_2} j & j_1 > j_2 \end{cases} \quad (16)$$

When $j_1 \leq j_2$, $j_1 \in \{0, \dots, n-1\}$, $j_2 \in \{0, \dots, n-j_1\}$; otherwise $j_1 \in \{1, \dots, n-1\}$, $j_2 \in \{0, \dots, j_1\}$.

Here the equivalence between the coordinates of the quantum gate and the positions of the elements of the weight matrix is established, then the coordinates of the quantum gate can be confirmed by retrieving the positions of the corresponding elements.

Step 9: Combined measurements. This step is measured with skill. Choosing the full output qubit of Eq. (15) and one of the qubits in Eq. (14), the corresponding word vector can be formed, which also conforms to the reality that the output has 1 more dimension than the input. If the dimensionality is to be guaranteed to be the same, a layer of neural network can be used.

V. EXPERIMENT AND DISCUSSION

This section implements the simulation of QSAN using IBM Qiskit and pennylane.

Preparation Currently qubits are severely limited, so an attempt is made to verify the feasibility of this scheme with a small homemade data sample. Firstly, 2 classical word vectors follow Transformer's practice and form a new set of samples by positional encoding [1]. Each new sample is re-characterized with 2 qubits as the input of QSAN.

Training Once the simple dataset is available, QSAN starts randomly assigning initial angles. It then carries out training following the quantum natural gradient training rule instead

of the classical gradient descent law [26]. The expectation function in this paper is defined as

$$\langle A \rangle = \langle \theta | H | \theta \rangle$$

where the Hamiltonian H is equal to $Z_2 Z_3 Z_4 Z_5$ (the subscript here indicates the line number of the quantum circuit), that is, the expectation on the Pauli operator Z for the observation of lines 2 to 5. The outcomes of quantum natural gradient descent and gradient descent training are shown in Fig. 8. In Fig. 8, the first figure explains the convergence of QSAN during the training process, concluding that the quantum natural gradient descent method converges faster and helps avoid the optimization from falling into local minima. The second figure shows the evolution of the 12 parameter angles during quantum natural gradient descent.

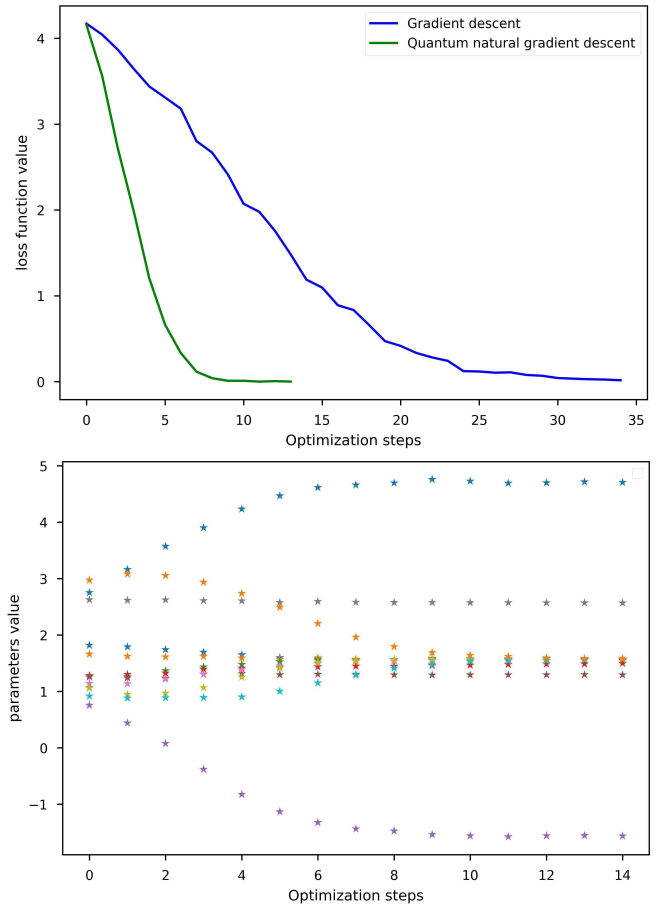


Fig. 8: Training results of QSAN: max_iterations = 500; conv_tol = 1e-06; step_size = 0.115

QBSASM Due to the extension of the classical attention score to a quantum state, the QBSASM is thus formed, giving the classical attention score a probabilistic character while being higher in dimensionality. At first, the self-attentive fraction presents a random state due to the random assignment of the initialization angle, as shown in the upper part of Fig. 9. After the quantum natural gradient descent, in the last round, a completely new attention distribution is obtained

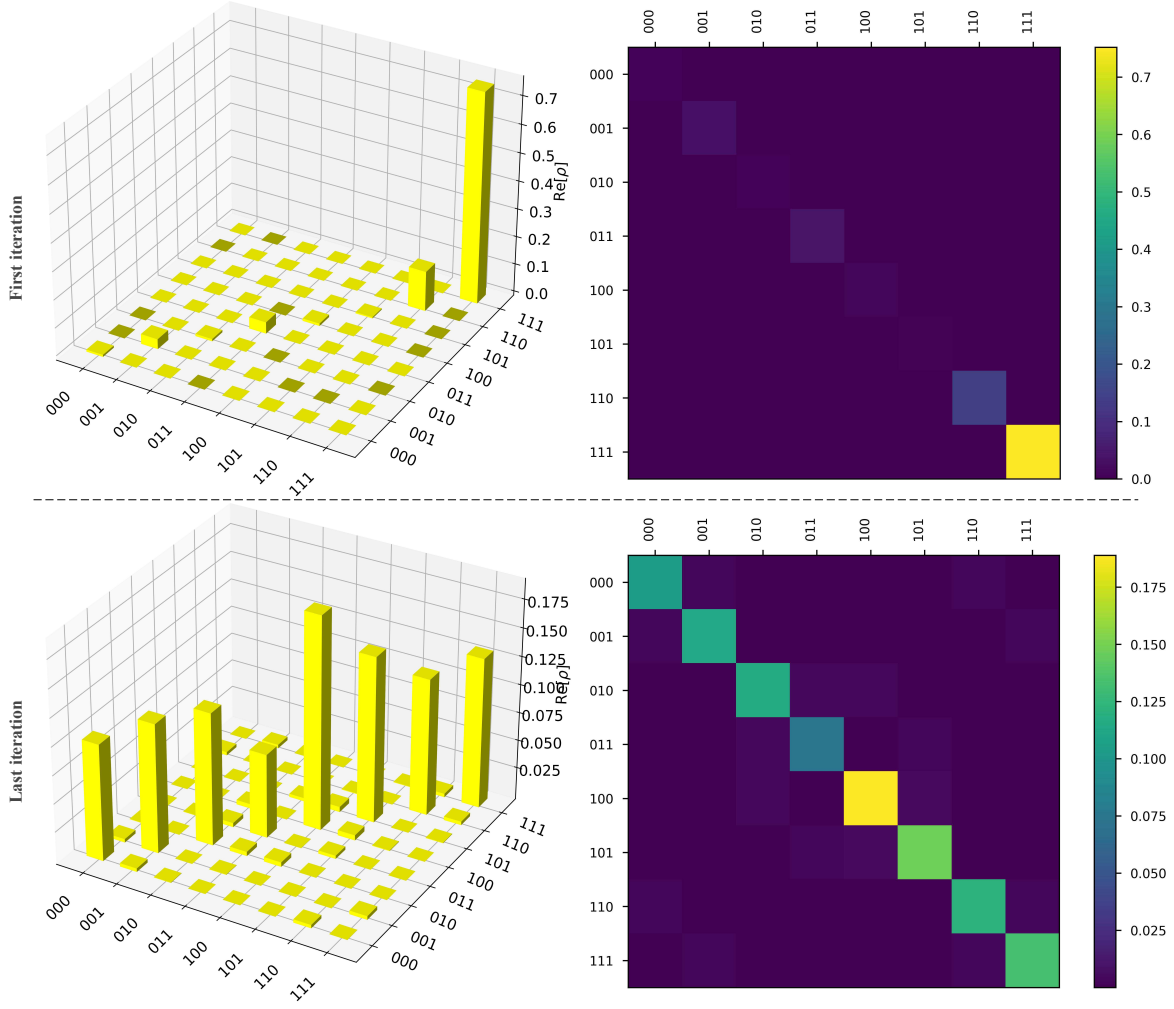


Fig. 9: Quantum attention score matrix

by intercepting this matrix, as in the lower part of Fig. 9. It is worth mentioning that the specific scores need to be known by measurement due to the presence of probabilistic properties, which means that by measurement, the QBSASM also collapses to some specific classical attention score matrix.

Discussion QSAN is difficult for ordinary computers to emulate because just one QBSASM consumes a large amount of storage, which is the storage advantage of quantum computers. In addition, QSAN uses logical operations between qubits instead of taking quantum numerical operations, which helps to save the qubits needed to build QSAN.

However, whether more qubits can be saved for QSAN is an open question. Quantum coordinates are utilized in the paper, and since it can facilitate the construction of quantum networks with similar structure repetition, whether it will be a subject of further optimization of the structure is worthy of deeper investigation. Establishing a complete theoretical system of quantum coordinates, and a series of coordinate operations, decomposition, and merging laws may give a more concise form to QSAN.

Further, QSAN, as an important component of machine learning, is merging with machine learning models, such as forming the new Quantum Transformer. whether Quantum

Transformer will have a secondary acceleration to the classical model is the next topic of this paper.

VI. CONCLUSION

SAM is investigated in the context of quantum computing. QSAM is a quantum insight of SAM with the quantum features of linearity, probability and reversibility. As the core of QSAM, QLS on the one hand redefines the classical inner product form of attention scores into a logical form, enabling its full deployment and thorough execution on quantum computers. On the other hand it is able to avoid numerical operations and save more auxiliary quantum bits. The by-product QBSASM is a density matrix expression of QLS that can be sampled to observe the attention distribution of the quantum system on the output. Finally, QSAN is the practice guided by QSAM. Subject to the current limited number of qubits, a miniaturized experiment demonstrates that QSAN can be trained faster as well as can redistribute weights on the output, proving effectiveness and feasibility.

ACKNOWLEDGMENT

We would like to thank all the reviewers who provided valuable suggestions.

REFERENCES

- [1] Ashish Vaswani, Noam Shazeer et al., “Attention is all you need,” in Proceedings of the 31st International Conference on Neural Information Processing Systems, 2017, pp. 6000–6010.
- [2] Tao Shen, Tianyi Zhou et al., “Disan: Directional self-attention network for rnn/cnn-free language understanding,” in Proceedings of the AAAI Conference on Artificial Intelligence, 2018, pp. 5446–5455.
- [3] Naihan Li, Shujie Liu et al., “Neural speech synthesis with transformer network,” in Proceedings of the AAAI Conference on Artificial Intelligence, 2019, pp. 6706–6713.
- [4] J. Fu, J. Liu et al., “Dual attention network for scene segmentation,” in 2019 IEEE/CVF Conference on Computer Vision and Pattern Recognition (CVPR), 2019, pp. 3141–3149.
- [5] Yunyang Xiong, Zhanpeng Zeng et al., “Nyströmformer: A nyström-based algorithm for approximating self-attention,” in Proceedings of the AAAI Conference on Artificial Intelligence, 2021, pp. 14138–14148.
- [6] Krzysztof Marcin Choromanski, Valerii Likhoshesterov et al., “Rethinking attention with performers,” in International Conference on Learning Representations, 2020.
- [7] Y. Kashiwagi, E. Tsunoo et al., “Gaussian kernelized self-attention for long sequence data and its application to ctc-based speech recognition,” in ICASSP 2021 - 2021 IEEE International Conference on Acoustics, Speech and Signal Processing (ICASSP), 2021, pp. 6214–6218.
- [8] Nikita Kitaev, Lukasz Kaiser et al., “Reformer: The efficient transformer,” in International Conference on Learning Representations, 2019.
- [9] Rewon Child, Scott Gray et al., “Generating long sequences with sparse transformers,” arXiv preprint arXiv:1904.10509, 2019.
- [10] Aurko Roy, Mohammad Saffar et al., “Efficient content-based sparse attention with routing transformers,” Transactions of the Association for Computational Linguistics, vol. 9, pp. 53–68, 2021.
- [11] Yuhui Yuan, Lang Huang et al., “Ocnet: Object context for semantic segmentation,” International Journal of Computer Vision, vol. 129, no. 8, pp. 2375–2398, 2021.
- [12] S. Zhuoran, Z. Mingyuan et al., “Efficient attention: Attention with linear complexities,” in 2021 IEEE Winter Conference on Applications of Computer Vision (WACV), 2021, pp. 3530–3538.
- [13] Michael Hahn, “Theoretical limitations of self-attention in neural sequence models,” Transactions of the Association for Computational Linguistics, vol. 8, pp. 156–171, 2020.
- [14] Frank Arute, Kunal Arya, et al., “Quantum supremacy using a programmable superconducting processor,” Nature, vol. 574, no. 7779, pp. 505–510, 2019.
- [15] Han-Sen Zhong, Hui Wang et al., “Quantum computational advantage using photons,” Science, vol. 370, no. 6523, pp. 1460–1463, 2020.
- [16] Lars S. Madsen, Fabian Laudenbach et al., “Quantum computational advantage with a programmable photonic processor,” Nature, vol. 606, no. 7912, pp. 75–81, 2022.
- [17] Man-Hong Yung, “Quantum supremacy: Some fundamental concepts,” National Science Review, vol. 6, no. 1, pp. 22–23, 2019.
- [18] Aram W. Harrow, and Ashley Montanaro, “Quantum computational supremacy,” Nature, vol. 549, no. 7671, pp. 203–209, 2017.
- [19] Xiaolei Niu, Yuexian Hou et al., “Bi-directional lstm with quantum attention mechanism for sentence modeling,” in Neural Information Processing, Cham, 2017, pp. 178–188.
- [20] Qin Zhao, Chenguang Hou et al., “Quantum attention based language model for answer selection,” in Artificial Intelligence and Mobile Services – AIMS 2021, Cham, 2022, pp. 47–57.
- [21] Alberto Peruzzo, Jarrod McClean et al., “A variational eigenvalue solver on a photonic quantum processor,” Nature Communications, vol. 5, no. 1, pp. 4213, 2014.
- [22] Marcello Benedetti, Erika Lloyd et al., “Parameterized quantum circuits as machine learning models,” Quantum Science and Technology, vol. 4, no. 4, pp. 043001, 2019.
- [23] Lukasz Cincio, Kenneth Rudinger et al., “Machine learning of noise-resilient quantum circuits,” PRX Quantum, vol. 2, no. 1, pp. 010324, 2021.
- [24] Jonas M Kübler, Andrew Arrasmith et al., “An adaptive optimizer for measurement-frugal variational algorithms,” Quantum, vol. 4, pp. 263, 2020.
- [25] Ryan Sweke, Frederik Wilde et al., “Stochastic gradient descent for hybrid quantum-classical optimization,” Quantum, vol. 4, pp. 314, 2020.
- [26] James Stokes, Josh Izaac et al., “Quantum natural gradient,” Quantum, vol. 4, pp. 269, 2020.
- [27] Abhinav Kandala, Antonio Mezzacapo et al., “Hardware-efficient variational quantum eigensolver for small molecules and quantum magnets,” Nature, vol. 549, no. 7671, pp. 242–246, 2017.
- [28] Nikolay V. Tkachenko, James Sud et al., “Correlation-informed permutation of qubits for reducing ansatz depth in the variational quantum eigensolver,” PRX Quantum, vol. 2, no. 2, pp. 020337, 2021.
- [29] E. Farhi, J. Goldstone et al., “A quantum approximate optimization algorithm,” arXiv: Quantum Physics, 2014.
- [30] Stuart Hadfield, Zhihui Wang et al., “From the quantum approximate optimization algorithm to a quantum alternating operator ansatz,” Algorithms, vol. 12, no. 2, 2019.
- [31] M. E. S. Morales, J. D. Biamonte et al., “On the universality of the quantum approximate optimization algorithm,” Quantum Information Processing, vol. 19, no. 9, pp. 291, 2020.
- [32] John Preskill, “Quantum computing in the nisy era and beyond,” Quantum, vol. 2, pp. 79, 2018.
- [33] Guangxi Li, Xuanqiang Zhao et al., “Quantum self-attention neural networks for text classification,” arXiv preprint arXiv:2205.05625, 2022.
- [34] Harry Buhrman, Richard Cleve et al., “Quantum fingerprinting,” Physical Review Letters, vol. 87, no. 16, pp.

167902, 2001.

- [35] Dorit Aharonov, Vaughan Jones et al., “A polynomial quantum algorithm for approximating the jones polynomial,” *Algorithmica*, vol. 55, no. 3, pp. 395-421, 2009.
- [36] Carlos Ortiz Marrero, Mária Kieferová et al., “Entanglement-induced barren plateaus,” *PRX Quantum*, vol. 2, no. 4, pp. 040316, 2021.
- [37] Jarrod R. McClean, Sergio Boixo et al., “Barren plateaus in quantum neural network training landscapes,” *Nature Communications*, vol. 9, no. 1, pp. 4812, 2018.
- [38] Qiskit Development Team. “Realamplitudes documentation,” <https://qiskit.org/documentation/stubs/qiskit.circuit.library.RealAmplitudes.html>.
- [39] Qiskit Development Team. “Summary of quantum operations,” https://qiskit.org/documentation/tutorials/circuits/3_summary_of_quantum_operations.html.

This figure "ss.png" is available in "png" format from:

<http://arxiv.org/ps/2207.07563v2>

This figure "thumbnail.jpeg" is available in "jpeg" format from:

<http://arxiv.org/ps/2207.07563v2>